Characterization of Photoionization Intermediates via ab Initio Molecular Dynamics†

Emily A. A. Jarvis, Eyal Fattal, Antonio J. R. da Silva, and Emily A. Carter*

Department of Chemistry and Biochemistry, Box 951569, University of California, Los Angeles, California 90095-1569

Received: June 16, 1999; In Final Form: September 2, 1999

Ab initio molecular dynamics (AIMD) allows one to probe complex potential energy surfaces at finite temperatures. Here we extend this technique to the analysis of vertical excited states along ground-state AIMD trajectories. We illustrate this idea via comparison to the silver trimer anion photoionization experiments of Boo et al. (*J. Phys. Chem.* **1997**, *101*, 6688). This work displayed an aberrant trend in the ionization efficiency near threshold, which suggests the presence of an intermediate state resonance. We present an AIMD simulation at the complete active space self-consistent field level of the silver trimer anion photoionization to ground-state neutral silver trimer for several different basis set expansions. We have analyzed the excited-state manifold via multireference singles and doubles configuration interaction (MRSDCI) and complete active space second-order perturbation theory (CASPT2) calculations performed at representative points along the neutral silver trimer trajectories in order to discern the nature and relative energy of the intermediate excited-state probed in the experiment. We find an excited state that may coincide with the possible resonance state accessed by the ∼400 nm probe and a higher near-linear excited state that may have been accessed by the ∼270 nm probe in the photoionization experiments.

1. Introduction

Ab initio molecular dynamics (AIMD) simulations have been used over the past 15 years to study gas and condensed phase atomic level processes at finite temperature with considerable success.[2,3] In particular, many processes involve complex rearrangements of atoms that defy our ability to construct analytical potential functions that correctly describe the essential physical interactions. It is for these systems that AIMD provides a crucial advantage: one computes the forces on the atoms "on the fly" for a classical dynamics simulation without ever fitting a potential function. Recently, there have been extensions of this adiabatic dynamics technique to following nonadiabatic dynamics on ab initio potential energy surfaces.[4] In the current paper, we propose another use of this technique, namely to use the conventional, adiabatic AIMD to follow the time-dependent evolution of a ground electronic state simultaneous with characterizing vertical excited states that would be accessible in a pump−probe photoionization experiment. We illustrate this application of AIMD on a simple system that has been studied experimentally and shows dramatic changes in structure upon photoionization. This is the Ag_3 anion−neutral−cation photoionization experiment.

Experimental[1,5−7] and theoretical[8−12] work has attempted to gain insight into the potential energy surfaces of the Ag_3^-, Ag_3, Ag_3^+ system and to elucidate the nature of Ag_3 excited states. The potential energy surface (PES) of the neutral Ag_3 is thought to be that of the "Mexican hat" form, similar to one described for Na_3.[5,13] Although much of the incentive for the study of small silver clusters is motivated by fundamental research, understanding the properties of silver clusters may also impact practical applications such as photography[14−16] and catalysis.[17,18]

Femtosecond pump−probe negative ion to neutral to positive ion (NeNePo) spectroscopy was introduced by Wolf et al.[5] in their study of the Ag_3^-−Ag_3−Ag_3^+ system. They related positive ion signal intensity, as a function of delay between pulses, to a measure of the evolving Franck−Condon factor for photoionization of the neutral, prepared by vertical detachment from a negative ion low vibrational state. With this technique, Wolf et al. hoped to probe the neutral molecule's vibrational motion. Their measurements were atypical of a simple time-dependent vibrational spectrum, with internal rearrangement dynamics possibly dominating the spectra. They interpreted the results to indicate time evolution of the Franck−Condon overlap and that the vibrational excitation energy was high enough to allow the neutral molecule to pseudorotate through the three equivalent equilibrium structures (the trough of the "Mexican hat" PES). The Wolf experiments detected positive ion signal and used ∼400 nm excitation. Boo et al. improved upon this NeNePo technique by introducing an enhanced detection method, whereby they were able to detect both positive ion and neutral products. Furthermore, they performed excitations in both the ∼400 and ∼270 nm regions. As a result, the Boo et al. measurements allow a more intricate interpretation of the general features found in the Wolf et al. experiments.[1] There is some discrepancy between the ensemble temperature of the two experiments, with a Wolf et al. experimental temperature of ∼300 K and the Boo et al. experiment taking place at much lower temperatures (∼40 K)[19] due to the supersonic expansion and a liquid nitrogen cooled ion source.

The NeNePo experiments displayed a strong dependence between photon energy and the time scale of the cation signal peak maximum. In the Boo et al.[1] experiments, the signal maximum using 410 nm pump−probe photons occurred at 1.0 ps, whereas photoionization using 396 nm excitations resulted in a cation signal maximum at ∼0.6 ps. Boo et al. proposed that the detailed shape of the cation signal might be largely

† We dedicate this paper to Professor William A. Goddard III, the master of extracting general concepts and specific insights from ab initio theory and of drawing connections to "real world" applications.

* Person to whom correspondence should be addressed.

10.1021/jp9919866 CCC: $19.00
Published on Web 11/20/1999

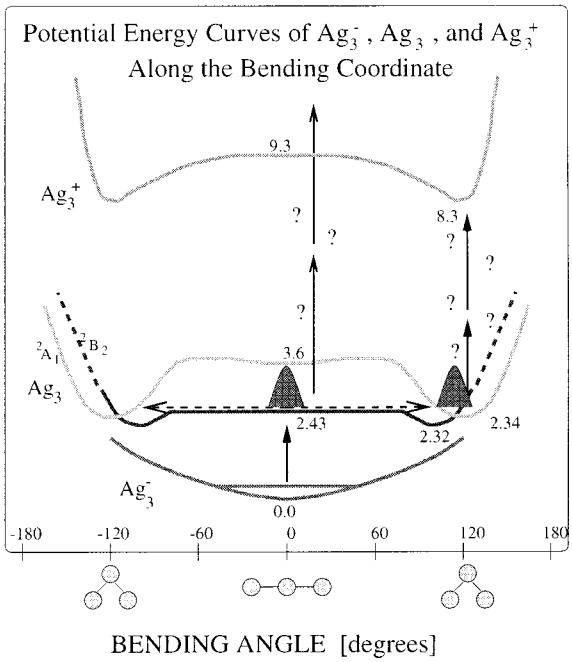

Figure 1. Schematic potential energy surfaces for Ag_3^-, Ag_3, and Ag_3^+. The numbers are the energy (eV) relative to the anion ground-state minimum.

affected by the role of an intermediate state resonance in this region. Experimental results from the third harmonic probe wavelength led Boo et al. to consider the possibility of a second resonance state, in the region of 4.5 eV with a linear structure, which could account for the lack of time delay in the cation signal at this probe energy.

Figure 1 shows a compilation (similar to one shown in the Boo et al. paper[1]) of Ag_3^-, Ag_3, Ag_3^+ potential energy surfaces taken from previous theory and experiment.[20−27] As this figure illustrates, the equilibrium structure of Ag_3^- is linear, minimizing electron repulsion between the two valence electron pairs. Upon vertical electron detachment, the linear triatomic finds itself near a saddle point on the neutral PES and immediately begins relaxing toward an isosceles triangle minimum. The Ag_3 cation, having only two valence electrons, adopts an equilateral triangle structure as its most stable configuration. This is due to the valence electronic structure, where the two electrons occupy a molecular orbital that is a totally symmetric combination of s-orbitals. The energies and electronic structure of Ag_3 excited states will be discussed in further detail in our results.

In 1996, Jeschke et al. presented a semiempirical molecular dynamics study designed to simulate the dynamics of Ag_3 clusters immediately after Ag_3^- photoionization.[28,29] They investigated the time scale necessary for linear Ag_3 to change to the obtuse triangular potential energy minimum and compared results for several temperatures, ranging from 29 to 1048 K.[28] The results showed strong temperature dependence. These dynamics studies were performed to explore the results of Wolf et al.'s NeNePo experiments and were prior to the Boo et al. study.

More recently, Hartmann et al. presented a multistate dynamics study of the Ag_3^-−Ag_3−Ag_3^+ system on a time scale of nuclear motion to simulate the NeNePo experiments.[10,11] Using ab initio CI calculations to compute points on the neutral and cation surfaces and coupled cluster (CCSD(T)) calculations to compute points on the anion surface, Hartmann et al. obtained precomputed grids on which to perform their classical MD simulations. They employed a one-electron relativistic effective core potential, accounting for core-valence correlation, along with an atomic basis described in another study.[32] Their dynamics were performed at 50 and 300 K in order to simulate conditions present in the Boo et al. and Wolf et al. experiments, respectively. From their dynamics, Hartmann et al. concluded that intracluster vibrational relaxation, in addition to structural relaxation, could play a large role in the dynamics. They also showed that dissipative intracluster vibrational relaxation and vibrational equilibration are viable in Ag_3 with excess vibrational energies associated with an equilibrium temperature of ∼1400 K. Furthermore, this study investigated how vibrational coherence, termination of intracluster vibrational relaxation, and change in geometry can be explored from the experimental data of the NeNePo experiments. From their simulations, Hartmann et al. predicted an increase in the time required for the appearance of the cation signal peak maxima with increased probe energy; however, the experimental data did not all fit within this prediction. Despite the fact that only one electron per atom was treated, the dynamics of Hartmann et al. contained a great deal of information and presented a compelling example of theory complementing and enriching experimental findings. Unfortunately, certain differences in the experimental data of Wolf et al. and Boo et al. were not fully reconciled by the simulations, although it seemed likely that temperature differences may be a primary cause of the discrepancies.[11] The power spectra of Ag_3 obtained by Hartmann et al.[10] showed strong temperature dependence, as the dynamics of Jeschke et al. also displayed.[28] Hartmann et al. also conjectured that certain discrepancies between the Boo et al. experimental data and the dynamics predictions might result from possible intermediate electronic resonance states.[10]

In the past few years, several experimental studies have interrogated the excited states of Ag_3. An early study investigating vibronic spectroscopy and some dynamics of neutral Ag_3 was performed several years prior to the NeNePo experiments by Cheng and Duncan.[20] Handschuh et al. obtained photoelectron spectra of Ag_n^- clusters. For Ag_3^-, they found a vertical ionization potential (IP) of 2.43 eV and several neutral excited states at linear geometry, which had energies of 1.19, 2.40, 3.14, 3.37, and 3.67 eV above the ground state.[6] Okazaki et al.[7] performed optical emission studies of Ag_3 clusters, observed the $^2A'_1$ excited state to the $^2B_2$ ground-state transition, and derived certain vibrational spectroscopic constants for neutral Ag_3. This study saw a need for further experiments to help elucidate, more precisely, the geometry and nature of the neutral Ag_3 ground state. Wedum et al.[30] and Wallimann et al.[31] investigated the absorption spectrum of Ag_3 employing extensive parameter fitting incorporating linear and quadratic Jahn−Teller coupling, as well as spin−orbit coupling. The more recent Wallimann et al.[31] study concluded that spin−orbit splitting is effectively quenched below the Jahn−Teller localization energy (about 300 cm^{-1} above the minimum) and may rise to values on the order of 10 cm^{-1}.

Despite the small size of Ag_3, its 141 electrons require use of an effective core potential (ECP) to make high level calculations feasible. Several relativistic effective core potentials (RECPs) for silver are available that treat explicitly one electron,[32] 11 electrons,[12,33] and 19 electrons.[33] In addition to these, a less commonly used 17e-RECP also exists.[34] Most of these are Hartree−Fock-based, but the most recent 11-electron[12] RECP was optimized at a correlated level of theory. The 11e- and 19e-RECP by Hay and Wadt (HW) used an all-electron numerical relativistic Hartree−Fock (one-component Cowan−Griffin formalism) calculation as the starting point for their effective core potentials. The 4d,5s,5p orbitals were created from

the lowest energy multiplet of the configurations $5s^14d^{10}$ and $5p^14d^{10}$. The f orbitals, necessary for creating the f potential, were obtained from the field of the nucleus plus the core orbitals on f^1. The 19e-RECP explicitly treats the outer core s and p orbitals, which can be valuable for metallic and cationic systems since the 4s and 4p orbitals may have similar radial extent to the 4d.[33] The recent Bonacic-Koutecky (BK) et al. 11e-RECP used the HW 11e-RECP as a starting point for their potential.[12] They then optimized their parameters by root-mean-square minimization of various CI and SCF calculated properties with respect to atomic experimental[35] and Dirac−Fock data,[36] followed by reoptimization according to silver dimer and atomic properties.[12] As a result, the BK 11e-RECP agrees more closely with experiment for a number of atom and dimer properties calculated at the multireference (doubles) configuration interaction (MRD-CI) and coupled-cluster singles and doubles (CCSD) levels.

Several theoretical studies of electronic excitations in Ag_3 have been reported previously. In general, these have been limited to investigating the molecule at its optimum geometry with imposed symmetry constraints. In 1981, Basch performed a CI study, with no d electron correlation, of Ag_3 clusters using his own 11e-RECP, which is reported in his paper.[8] Subsequently, Walch performed single reference externally contracted CI calculations that did include d electron correlation and added diffuse functions to better describe the Rydberg states. He used the HW 11e-RECP[33] and a valence basis described in one of his previous papers.[22] More recently, Bonacic-Koutecky et al. performed MRSDCI calculations to find stabilities and ionization potentials of small Ag clusters using a 1e-RECP designed to account for core-valence correlation effects.[32] In another study, Bonacic-Koutecky et al. investigated Ag_3 excited states using an equation-of-motion coupled-cluster method with their new BK 11e-RECP.[12] The spectra obtained in these studies were quite diverse and will be more thoroughly discussed in the results.

In this paper, we first describe the AIMD trajectories, which simulate photoionization (Ag_3^- to Ag_3) experiments. The studies by Hartmann et al. had already explored extensive dynamics on this system.[10,11] A drawback of our ab initio dynamics is that, due to computational time constraints, only a limited number of trajectories can be performed. Accordingly, we cannot claim that our dynamics represents a true statistical sampling; nevertheless, we do obtain a "random" yet representative sample of time-evolving Ag_3 states upon electron photodetachment of the anion. In turn, we chose various points along these time-evolving states at which we performed MRSDCI and CASPT2 calculations. By solving for multiple eigenvalues in these calculations, we extract the time-evolving Ag_3 electronic state spectrum, and by exploring the configurations and associated configuration interaction (CI) coefficients for each state (in relation to the ground state) we characterize the primary contributing excitations as a function of time.

2. Computational Details

Although optimum structures have been computed at various levels of theory previously, we performed our own geometry optimizations on the silver clusters for each basis set and RECP used. Since the AIMD simulations should not involve symmetry constraints, we did not impose symmetry, bond angle, or bond length constraints in our minimizations. The geometries were first optimized at the generalized valence bond with perfect pairing (GVB-PP)[37] level using the program Jaguar[38] and then further refined at the complete active space self-consistent field (CASSCF)[39] level with the HONDO code.[40]

Our AIMD code is designed to propagate the atomic nuclei as classical particles using ab initio forces in Newton's equations of motion (evaluated by the velocity-Verlet integrator[41]). In particular, we used Born−Oppenheimer AIMD for our trajectories, meaning the wave function was converged to the Born−Oppenheimer surface at each time step.[42] These dynamics were performed at the CASSCF level for the anion and neutral trajectories using the 19e-RECP and the two 11e-RECPs[12,33] described earlier. In each case, the active space consisted of the valence 5s electrons in three or four orbitals for the neutral and anion, respectively.

Most trajectories were performed using a time step of 9.7 fs, which was found to conserve energy to at least 1.0×10^{-3} eV for the ~2 ps neutral trajectories. Several neutral trajectories were performed with 1.2 and 4.8 fs time steps, which displayed similar energy conservation. The anion easily conserved energy to at least 1.0×10^{-4} eV for ≥3 ps with a 9.7 fs time step.

Initially, we equilibrated the anion for ~0.3 ps by uniformly scaling the velocities of each atom at any time step in which the molecule was not within 20 K of the target temperature. The initial velocities were taken from a Boltzmann distribution at 40 K, while the initial coordinates were those of the optimized anion structure. Most anion trajectories were initially equilibrated to a target temperature of 40 K to reflect conditions in Boo et al.'s NeNePo experiment.[1] After this initial velocity scaling, the system was allowed to freely propagate (no symmetry or velocity constraints) for ≥3 ps. Two anion trajectories were created for each basis set and RECP considered. Neutral trajectories were started as vertical ionization points along the anion trajectories and were separated by at least 0.2−0.5 ps to be statistically independent. Eight of these neutral trajectories were performed with the HW 11e-RECP, five were performed with the HW 19e-RECP, and three BK 11e-RECP trajectories were produced. All neutral trajectories were allowed to freely propagate ≥1.5 ps. No dynamics were performed for the cation. However, the energy of the optimized cation structure was calculated to allow ionization potential (IP) comparisons with other studies, and we calculated the MRSDCI (32 correlated electrons) and CASPT2 (2 active electrons and orbitals) cation ground-state energy for the vertical ionization points along the neutral trajectories.

MRSDCI excitation spectra for Ag_3 were calculated with no symmetry constraints using the CAS (3 electrons/3 orbitals) as the reference space. Using the two HW basis-RECPs (11 and 19 electrons), we imposed no restrictions on reference space configurations to calculate the eight lowest eigenvalues of the neutral molecule. The convergence for the 19e-RECP was much faster and smoother than that observed for the two 11e-RECPs.

We observed significant improvement (0.6 eV) in the agreement between calculation and experiment for the adiabatic IP of Ag_3^- when we correlated 33 electrons, rather than correlating only three electrons, at the MRSDCI level with the HW 11e-RECP. As a result, in all of our MRSDCI calculations, we chose to correlate 33 electrons (which includes the 4d and 5s electrons for each atom).

CASPT2[43] (Møller−Plesset) calculations solving for the eight lowest energy levels were performed using the HW and BK 11e-RECPs. As before, the CAS (5s electrons in 5s orbitals) comprised the reference space of our calculations; however, excitations from the 4d orbitals were not included since we found that the d excitations played only a minor role in the eight lowest roots from the MRSDCI calculations. Naturally, these calculations were very quick compared to MRSDCI, and although the level of theory for CASPT2 is much lower than

TABLE 1: IP Results from Theory and Experiment

	experiment[a]	11e (H-W)[b] MRSDCI	11e (H-W)[c] CASPT2	11e (B-K)[d] CASPT2	19e (H-W)[e] MRSDCI	Basch[f] SDCCI	Walch[g] SDCCI	1e B-K[h] FCI	11e B-K[i] CCSD
Ag_3^- to Ag_3									
vertical	2.43	1.66	2.82	2.03	1.61	1.40		2.45	
adiabatic	2.32	1.56	2.73	1.12	1.51	1.08		2.10	
Ag_3 to Ag_3^+									
adiabatic	~6.0	4.78	5.54	5.76	4.77	4.62	4.81	5.61	5.18

[a] See description in Boo et al.[1] and refs 20, 21, and 24−26. [b] MRSDCI results for 11e Hay-Wadt RECP with 33 correlated electrons at the CASSCF optimum geometry. [c] CASPT2 results for 11e Hay-Wadt RECP three electrons in three orbitals CAS. [d] CASPT2 results for 11e BK RECP three electrons in three orbitals CAS. [e] MRSDCI results for 19e Hay-Wadt RECP with 33 correlated electrons at the CASSCF optimum geometry. [f] SDCI with three correlated electrons.[8] [g] SDCCI for 11e Hay-Wadt RECP with 33 correlated electrons and additional Rydberg orbitals.[9] [h] Full CI with 1e BK RECP. [32] [i] Coupled cluster singles and doubles for 11e BK RECP.[12]

that of MRSDCI, numerous calculations have shown that CASPT2 calculations can supply valuable insight into spectra for a variety of systems.[44]

3. Results and Discussion

The optimized structures we found were similar to those reported previously by Walch et al.[9,22] and Bonacic-Koutecky et al.,[12,32] who used C_{2v} (neutral) and D_{3h} (cation) symmetries. With no imposed symmetry in our calculations, we found the minimum energy structures of the anion to be linear, the neutral to be an obtuse triangle, and the cation to be nearly an equilateral triangle. The energy of neutral Ag_3, at the CASSCF level, was fairly insensitive to bond angle changes of several degrees, especially for the 19e-RECP. This agrees with the relatively flat PES reported previously.[8,26]

As a means to compare our results with other theoretical and experimental values, we calculated vertical and adiabatic IP values for Ag_3^- and Ag_3 described with the HW basis sets and RECPs. We also explored the effects of adding diffuse s and p functions to our basis; however, those trial atomic bases displayed negligible improvements in IP values for MRSDCI calculations with three correlated electrons. Table 1 displays our IP predictions as well as several other results from theory and experiment. Explicit inclusion of the outer core electrons does not improve the predicted IP value for Ag_3 from our MRSDCI calculations with 33 correlated electrons (although there was some fortuitous improvement when only three electrons were correlated). Although the IP from our MRSDCI calculations is underestimated, we reproduce the energy differences between the linear and equilateral triangle on the cation surface quite well at this level of theory (1.29 eV compared to an experimental estimate of ~1 eV[25]). The fair agreement between our CASPT2 IP and experimental values suggests that this may be a reasonable level at which to address excitation energies for Ag_3.

Figure 2 displays the results of our MRSDCI calculations at structures optimized at the CASSCF level using HW 11e- and 19e-RECPs as well as results from the Basch, Walch, and Bonacic-Koutecky et al. calculations.[8,9,12] Both the Walch and Basch calculations used single reference single and double excitation CI. The Walch ground-state Ag_3 had C_{2v} symmetry, and the excited states assumed D_{3h} symmetry. The Walch and Bonacic-Koutecky et al. calculations included 5s and 4d excitations, while the Basch calculations excluded the 4d excitations. The Bonacic-Koutecky et al. work used C_{2v} symmetry for the neutral states and employed equation-of-motion coupled cluster calculations. Some variation in these predicted spectra is expected due to the differences in calculation levels, basis set and RECP, and symmetries employed in the calculations. Although these predicted spectra differ, each exhibits at least one state between 2.4 and 3.0 eV. Our results, and those

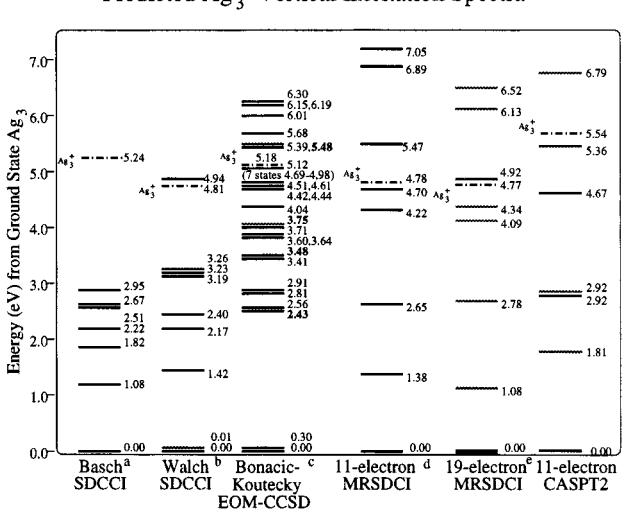

Figure 2. Spectra of Ag_3 from SDCI, EOM-CCSD, and MRSDCI. The Ag_3^+ level is indicated by a dash−dotted line. [a]SDCI with three correlated electrons.[8] [b]SDCCI for 11e Hay-Wadt RECP with 33 correlated electrons and additional Rydberg orbitals.[9] [c]Equation-of-motion coupled cluster singles and doubles for the 11e BK RECP.[12] [d]MRSDCI with 11e Hay-Wadt RECP with 33 correlated electrons at the CASSCF optimum geometry. [e]MRSDCI with 19e Hay-Wadt RECP with 33 correlated electrons at the CASSCF optimum geometry. [f]CASPT2 results for 11e Hay-Wadt RECP three electrons in three orbitals CAS.

of Bonacic-Koutecky et al., predict two higher lying states within 1 eV below Ag_3^+ that were not shown in the previous calculations of Basch and Walch. It is likely that one of these states corresponds to the possible resonance state accessed by the ~270 nm probe in the Boo et al. experiment.

We were surprised to find some difference in the behavior of the three basis set/RECP descriptions when we performed low-temperature AIMD simulations on the neutral Ag_3. Figure 3 displays sample low-temperature neutral trajectories for each basis set/RECP considered. The 19e-RECP at ~40 K only bent to ~105° angles. The 11e-RECP of Bonacic-Koutecky showed even more reluctance to bending, merely bending ~35° from the linear structure. However, the neutral trajectories using the HW 11e-RECP explored a much wider range of bending angles at this low temperature, consistent with expected physical behavior for this system. Of course, at higher temperatures, corresponding to greater vibrational excitation of the neutral Ag_3 likely achieved in the photoionization experiments,[1,5] the trajectories for each basis set/RECP were able to access smaller angle structures and showed faster bending times. Recurrences of the linear neutral Ag_3 were not observed on the ~1 ps time scale of the Boo et al. experiment. Accordingly, our BK 11e-RECP trajectories showed unphysical behavior. As mentioned

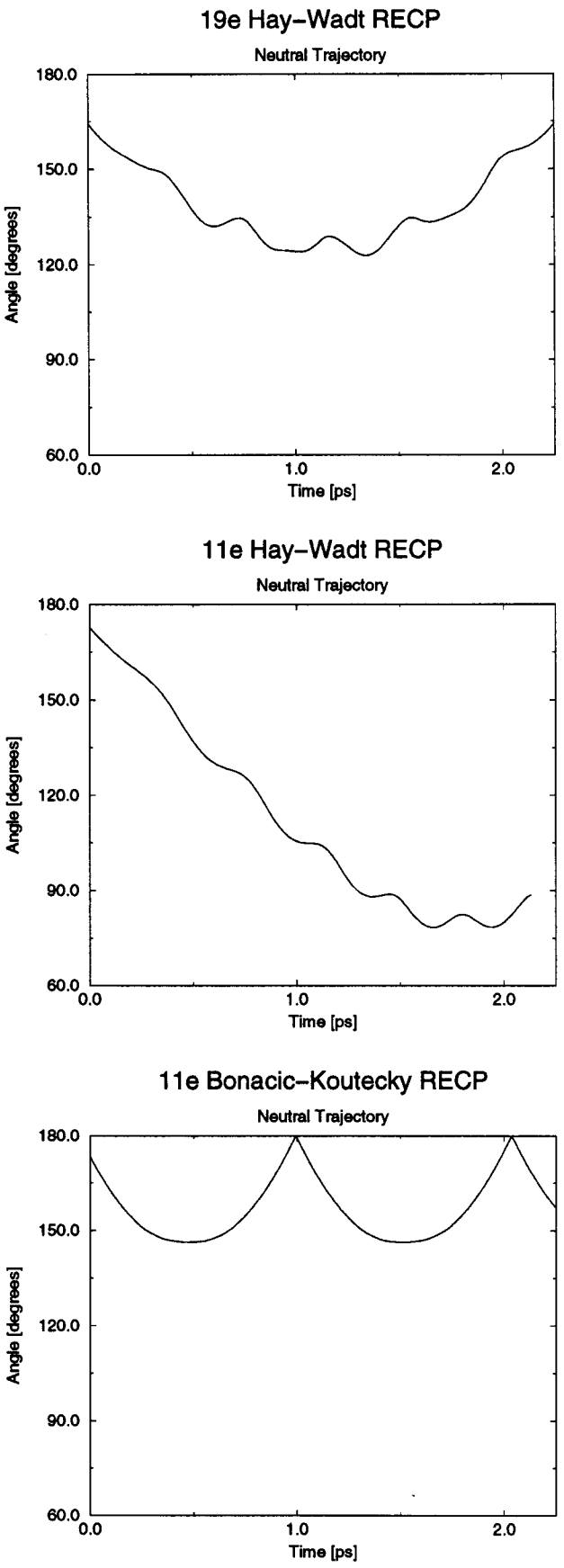

Figure 3. Bond angle of sample low-temperature (both Hay-Wadt RECP at 40 K, Bonacic-Koutecky RECP at 80 K) Ag_3 AIMD trajectories for three different basis sets/RECPs.

earlier, the 40 K temperature was employed on the basis of an estimate of the anion temperature.[19] Experimentally, the vertical

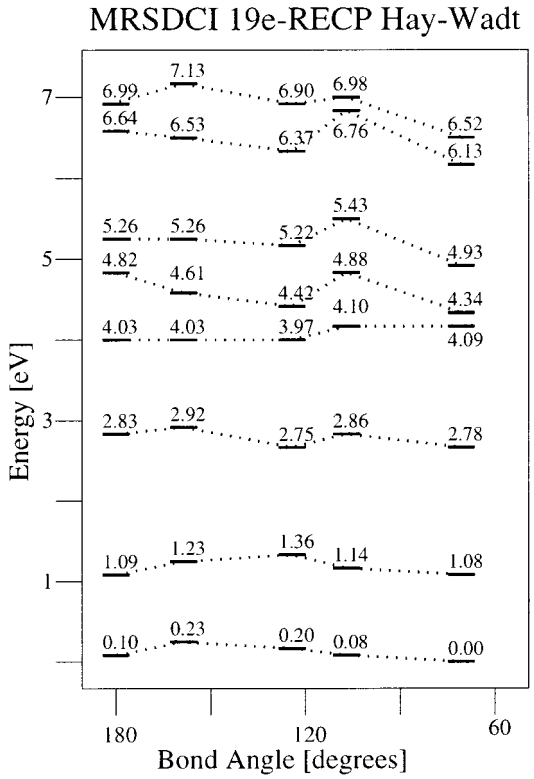

Figure 4. MRSDCI excitation spectra of Ag_3 for four bond angles along a neutral trajectory at 40 K (180° at <0.1 ps, 160° at 0.16 ps, 120° at 0.70 ps, and 108° at 0.9 ps) and at the optimized structure.

IP of Ag_3^- is thought to be 2.43 eV. The photon energies used in the Boo et al. experiment were considerably higher (~3 eV), but it is assumed that most of the excess energy would go into kinetic energy of the free electron rather than remaining in the neutral Ag_3. However, it is likely that many neutral trimers will be left vibrationally excited; hence, a simulation reflecting a higher effective temperature could be useful. Our MP2 estimates of the zero point energies for the four vibrational modes of the anion show that the thermal energy at 40 K is roughly equivalent to their sum. To further convince ourselves that we were effectively populating at least the zero point vibrational levels for each of the anion modes, we performed a few higher temperature (80 K) trajectory simulations as well; these were similar to the lower temperature trajectories, although they displayed faster bending times.

Figure 4 displays the 19e-RECP excitation spectra for four structures along a neutral Ag_3 trajectory as well as the optimized structure to include comparison with this smaller angle structure. In these spectra, it appears that most excited states are fairly insensitive to large changes in molecular bond angle. Note that although the bending angle varies in the trajectory, the bond lengths generally stayed within 10% of their optimum value. Independent of the structure, we observe three states below 3 eV. Given the minor differences observed between the 19e and 11e treatments (see Figure 2), we then explored only the four lowest roots for further MRSDCI calculations with the 11e-RECP.

Figure 5a displays the four lowest roots of the excitation spectra using the 11e-RECP. The top dotted line shows the corresponding MRSDCI Ag_3^+ energy for each structure. The trend in decreasing IP with decreasing angle is consistent with the increased positive ion signal at later times observed in the NeNePo experiments with ~3 eV pump−probe photons. Indeed, the bending time scales are consistent with the peak in positive

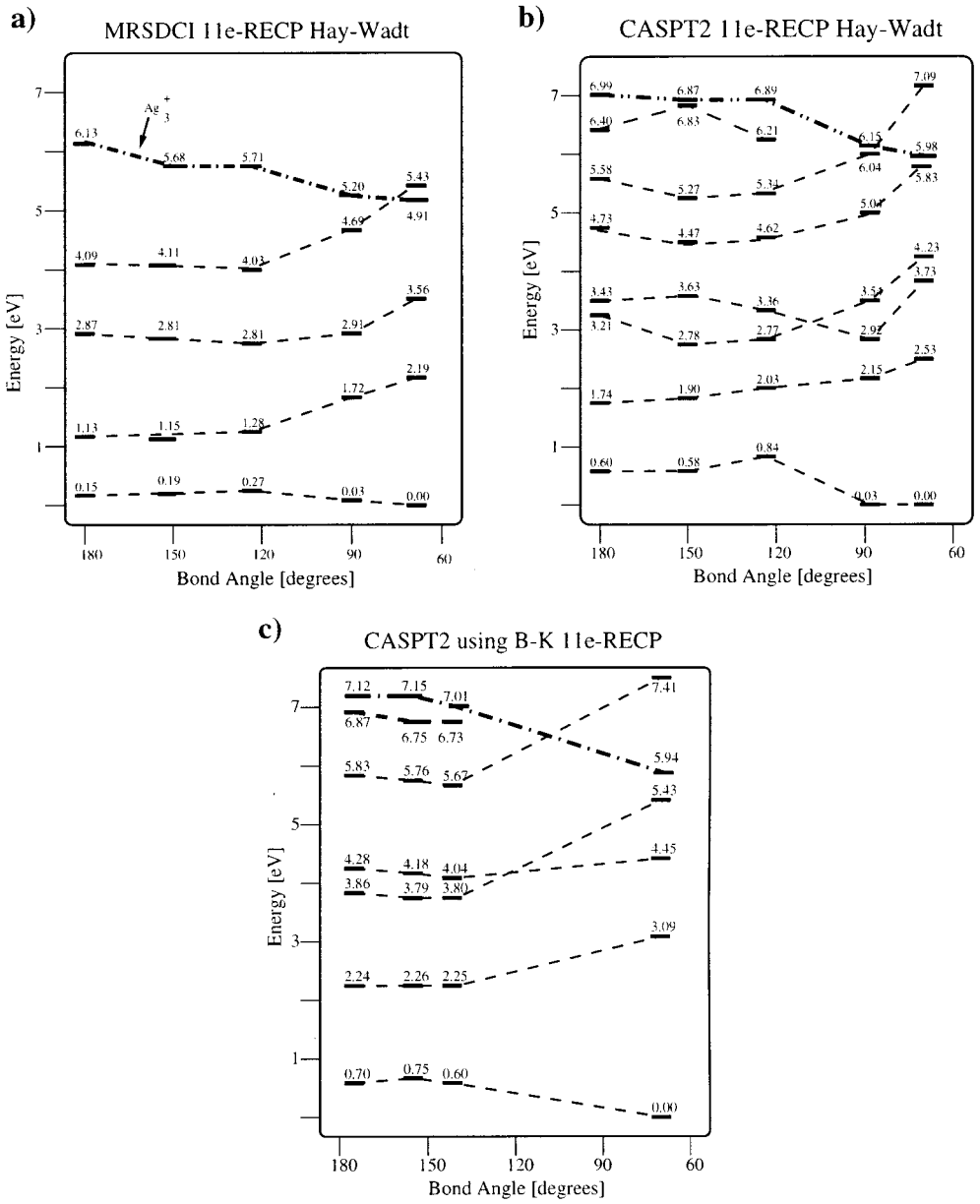

Figure 5. Excitation spectra of Ag_3 along neutral trajectories with cation energies (along dot−dashed line) also shown for each point. (a) MRSDCI excitation spectra of Ag_3 (Hay-Wadt) vs bond angle along a neutral trajectory at 40 K (180° at <0.1 ps, 150° at 0.35 ps, 124° at 0.78 ps, and 89° at 1.3 ps) and an optimized 70° structure. (b) CASPT2 excitation spectra of Ag_3 (Hay-Wadt) vs bond angle along a neutral trajectory at 40 K (same angles and times as in part a) and an optimized 70° structure. (c) CASPT2 excitation spectra of Ag_3 (Bonacic-Koutecky) vs bond angle along a neutral trajectory at 80 K (180° at <0.1 ps, 157° at 0.16 ps, and 146° at 0.5 ps) and the optimized structure.

ion signal at ∼1 ps using ∼400 nm photons. It is interesting to note that the minimum energies of several excited states using the HW 11e-RECPs occur at somewhat wider angles than the minimum energy ground-state structure. A structure with optimized bond lengths and a 70° bond angle is included as well. Although the optimum geometry at CASSCF level had a wider bond angle (80°), the ground-state energy for the 70° angle structure was lower at the MRSDCI and CASPT2 level. This 70° angle is similar to optimized Ag_3 structures from other studies.[9,12] The ∼180° structure is obtained upon ionization. Most of the ∼40 K trajectories would reach angles of ∼150° within 0.4−0.6 ps, ∼120° within 0.8−1.1 ps, and ∼90° within 1.3−1.8 ps. Higher temperature trajectories displayed faster bending times. A similar phenomenon was displayed in the dynamics with varying initial temperatures performed by Jeschke et al.[29] Figure 5b shows our CASPT2 results using HW 11e-RECP. This figure can be compared to the analogous MRSDCI spectrum.

The basis reported for the BK 11e-RECP by Bonacic-Koutecky et al.[12] was somewhat larger than that used for the Hay-Wadt examples. As a result, computational size constraints led us to explore only CASPT2 spectra, rather than MRSDCI, to investigate the excited states along the BK 11e-RECP trajectories. Figure 5c shows our CASPT2 results along one such trajectory and at the optimized structure. In attempts to obtain a wider variation in bending angle, the anion equilibration for this trajectory took place at 80 K; although, unfortunately, we were still only able to access ∼145° angle structures.

Although differences between the spectra are obvious, one characteristic common to all calculations is preserved: several excited states display wide-angle minima. The first two excited states of the linear structures from our MRSDCI calculations compare quite favorably with those found in the Handschuh et al. photoelectron spectra.[6] Unfortunately, in our calculations, we do not see all of the states they observed. The dotted lines in the CASPT2 figures show crossing of the second and third

excited states since the character of similar configurations contributing to the eigenvalue was not consecutive when comparing structures with >90° bending angle to those with smaller bending angle.

As shown, the excitation spectra we obtained displayed some sensitivity to geometry of the Ag_3. Although the neutral ground state energy appears relatively insensitive to bending angle change, from our MRSDCI calculations, some of the excited states appear more affected by this variation. It must be remembered that we are only comparing against bond angle here. Since our AIMD trajectories were performed without constraint, the bond lengths were also varying, although we cannot graphically display those changes here. The recent Bonacic-Koutecky et al. results for the Ag_3 excited states found that d electrons do not contribute to leading excitations in the intense transitions except for their high energy 8^2A_2 state at 5.48 eV.[12] The MRSDCI excited states we obtained from the Ag_3 wave functions taken along the neutral trajectories showed similar behavior, with d electron excitations comprising only minor contribution to the three or four highest energy states calculated. The several lowest eigenvalues were composed of only s electron transitions, primarily within the reference space, while the higher energy states had some contribution from d excitations; however, the CI coefficients corresponding to d electron excitations were generally below 0.08.

As was mentioned in relation to Figure 2, there are some discrepancies between predicted Ag_3 excitation spectra. This indicates a note of caution concerning expectations of accuracy vis-à-vis sensitivity to choice of method and basis set/RECP. Nevertheless, certain energy states from our results fit quite well with the possible resonance states mentioned by Boo et al.[1] The intermediate state resonance, which they possibly accessed at longer second harmonic wavelengths (≤3 eV), coincides with the second excited state obtained from our MRSDCI calculations. In all these calculations, the second state, slightly under 3 eV, is well-separated from the other states. Although the PES of that state appears to be fairly flat, the fact that it does not display a well-defined minimum at a linear structure is worth noting. Presumably, this relatively flat surface would allow the molecule to easily access a triangular structure. With single photon absorption from this state in the triangular region, the Ag_3 should be able to access the cation surface near its minimum. However, a more linear structure would not have enough energy, since the cationic PES has ∼1 eV difference in energy between linear and equilateral triangle structures, as reported previously,[25] and as shown by our cation energies from MRSDCI calculations (Figure 5a). The possible intermediate state Boo et al. accessed with 277 nm photons is less obvious from our excitation spectra since the 19e-RECP MRSDCI results showed several states energetically close to this region. The third excited state for the 11e-RECP MRSDCI calculations appears to be the most likely candidate. These results display an obvious increase in the energy of this state for smaller angle structures. Furthermore, its excitation energy of ∼4 eV above the ground state agrees fairly well with the ∼4.5 eV energy of the photon. This is especially compelling if one considers that the higher energy states in our calculations were quite possibly underestimated, as evidenced by our underestimated IP values. Qualitatively, our CASPT2 calculations showed similar results. They display a fairly flat state around 3−4 eV (where the energy separations are possibly overestimated) and a higher energy near-linear state, which would correspond to the resonance state accessed by the third harmonic probe excitations.

4. Conclusions

From our predicted Ag_3 excitation spectra along dynamical trajectories, it seems that the ∼3 eV possible "resonance state" described by Boo et al. consists primarily of an s to s transition within the valence orbitals. Likewise, the second possible resonance state at ∼4.5 eV is likely composed of similar s to s valence space excitations according to our calculations. We note, however, that our basis set was not designed to describe Rydberg states. Using the Rydberg formula approximation in Herzberg[45]

$$E_n = \mathrm{A} - \mathrm{R}/(n - \delta)^2$$

and δ values from Walch,[9] we estimate Rydberg excited states (for $n = 3, 4, 5$) that could energetically account for the resonance states accessed by the single photon probe excitations. However, the PESs of the Rydberg states obtained by this approximation will all mirror the rather steep PES of the cation, with minima approaching the equilateral triangle structure. Hence, although we cannot rule out the possibility that the resonance states are characterized by excitations to Rydberg orbitals rather than by primarily valence s excitations, within this admittedly crude approximation, these Rydberg states do not display the bent (lower resonance state) and near-linear (upper resonance state) minima anticipated by Boo et al.[1]

While our results provide strong qualitative evidence of the existence and nature of possible resonance states at the appropriate energies, we cannot quantitatively pinpoint the time-evolving energies of those states such that we could distinguish expected behavior between photon energies differing by ∼0.1 eV. Although our data cannot effectively elucidate the experimentally observed change in cation detection time scales with slight variations in wavelength, we do observe excited states that appear to match well those accessible at the photon energies used in the experiment. It seems plausible that the ∼3 eV probe photons are able to access the excited state we observe in this region. The Ag_3 would then be able to explore a variety of bending configurations along the fairly flat PES we observe for this state, and the time scale for this bending may be significantly affected by slight variations in the photon energy. The second ∼3 eV photon, required to reach the cation, would only supply enough energy when the molecule was bent to smaller angle structures due to the sharper angular dependence of the Ag_3^+ PES. The energy of the hypothetical linear state, experimentally anticipated at ∼4.5 eV by Boo et al.,[1] is possibly underestimated by our HW 11e-RECP MRSDCI calculations and could be somewhat overestimated by the CASPT2 calculations. Nevertheless, we find higher excited states, around the appropriate region energetically, which do display lower energies for wide-angled or linear structures. Furthermore, the excitations contributing to the characterization of this state are similar for both the MRSDCI and CASPT2 calculations. Detailed characterization, to explore the likelihood of vast differences in vibrational excitation of this state accessed by photons differing by 0.1 eV, would require more work from theory and possibly experiment.

The kinetic energy of the electron ejected upon photoionization of the anion is not measured in the NeNePo experiment. As mentioned before, it is expected that most of the photon energy, in excess of the vertical ionization energy, would be transferred to the electron. This is supported in the Hartmann et al. dynamics study by the narrow range (0.05 eV) of Franck−Condon factors for the vertical photodetachment energies.[11] Boo et al. conjectured that the change in cation detection time scales, according to the pump−probe wavelengths, was likely due to

an intermediate probe-accessed state rather than greater bending excitation from the photon serving as the pump. The dynamics of Jeschke et al.,[29] Hartmann et al.,[10,11] and the few higher temperature trajectories we performed showed obvious temperature dependence. Most dramatically, the Jeschke et al. results displayed appearance of triangular Ag_3 0.5 ps sooner for an initial temperature of 104 K than for 29 K, corresponding to only a 0.02 eV difference.[29] Accordingly, from the dynamics studies, it seems premature to assert that greater bending excitations have no involvement in the cation detection time scale disparity between 410 and 420 nm versus 390−396 nm pump photons. While our excitation spectra provide support for resonance state availablility at the appropriate energies, a more thorough investigation of temperature dependence would be useful for a more quantitative description of the experimental results.

We have presented an application of AIMD to the study of time-evolving excited-state spectra for the specific case of the neutral silver trimer. We have identified possible resonance states accessed in the NeNePo experiments and offered a theoretical confirmation for the nature of these states anticipated by Boo et al.[1] Likewise, our results qualitatively mirror the time dependence of the cation appearance peak maxima with ∼3 and ∼4.5 eV probe excitation. Although direct quantitative comparison between experiment and theory for the Ag_3 NeNePo experiments may not be possible at this time, it seems that theory can supply insight into the character of time-evolving excited states and provide useful qualitative information. This technique could be easily applied to explore the time evolution of excited-state manifolds for a variety of femtosecond−picosecond time scale experiments.

Acknowledgment. Financial support from the Office of Naval Research and the Army Research Office is gratefully acknowledged. We also thank Professor W. Carl Lineberger for calling our attention to this problem and for helpful discussions.

References and Notes

(1) Boo, D. W.; Ozaki, Y.; L. Andersen, H.; Lineberger, W. C. *J. Phys. Chem.* **1997**, *101*, 6688.
(2) Radeke, M. R.; Carter, E. A. *Annu. Rev. Phys. Chem.* **1997**, *48*, 243.
(3) Parrinello, M. *Solid State Commun.* **1997**, *96*, 107.
(4) Ben-Nun, M.; Martinez, T. J. *J. Chem. Phys.* **1998**, *108*, 7244.
(5) Wolf, S.; Sommerer, G.; Rutz, S.; Schreiber, E.; Leisner, T.; Wöste, L. *Phys. Rev. Lett.* **1995**, *74*, 4177.
(6) Handschuh, H.; Chia-Yen Cha; Bechthold, P. S.; Ganteför, G.; Eberhardt, W. *J. Chem. Phys.* **1995**, *102*, 6404.
(7) Okazaki, T.; Saito, Y.; Kasuya, A.; Nishina, Y. *J. Chem. Phys.* **1996**, *104*, 812.
(8) Basch, H. *J. Am. Chem. Soc.* **1981**, *103*, 4657.
(9) Walch, S. P. *J. Chem. Phys.* **1987**, *87*, 6776.
(10) Hartmann, M.; Pittner, J.; Bonacic-Koutecky, V.; Heidenreich, A.; Jortner, J. *J. Chem. Phys.* **1998**, *108*, 3096.
(11) Hartmann, M.; Heidenreich, A.; Pittner, J.; Bonacic-Koutecky, V.; Jortner, J. *J. Phys. Chem.* **1998**, *102*, 4069.
(12) Bonacic-Koutecky, V.; Pittner, J.; Boiron, M.; Fantucci, P. *J. Chem. Phys.* **1999**, *110*, 3876.
(13) Broyer, M.; Delacrétaz, G.; Labastie, P.; Wolf, J. P.; Wöste, L. *J. Phys. Chem.* **1987**, *91*, 2626.
(14) Fayet, P.; Granzer, F.; Hegenbart, G.; Moisar, E.; Pishel, B.; Wöste, L. *Phys. Rev. Lett.* **1985**, *55*, 3002.
(15) Flad, J.; Stoll, H.; Preuss, H. *Z. Phys. D* **1987**, *6*, 193, 287.
(16) Mostafavi, M.; Marignier, J. L.; Amblard, J.; Belloni, J. *Z. Phys. D* **1989**, *12*, 31.
(17) Carter, E. A.; Goddard, W. A., III. *J. Catal.* **1988**, *112*, 80.
(18) Carter, E. A.; Goddard, W. A., III. *Surf. Sci.* **1989**, *209*, 243.
(19) Lineberger, W. C. Private communication.
(20) Cheng, P. Y.; Duncan, M. A. *Chem. Phys. Lett.* **1988**, *152*, 341.
(21) Flad, J.; Igel-mann, G.; Preuss, H.; Stoll, H. *Chem. Phys.* **1984**, *90*, 257.
(22) Walch, S. P.; Bauschlicher, C. W., Jr.; Langhoff, S. R. *J. Chem. Phys.* **1986**, *85*, 5900.
(23) Balasubramanian, K.; Liao, M. Z. *Chem. Phys.* **1988**, *127*, 313.
(24) Balasubramanian, K.; Feng, P. Y. *Chem. Phys. Lett.* **1989**, *159*, 452.
(25) Partridge, H.; Bauschlicher, C. W., Jr.; Langhoff, S. R. *Chem. Phys.* **1990**, *175*, 531.
(26) Ho, J.; Ervin, K. M.; Lineberger, W. C. *J. Chem. Phys.* **1990**, *93*, 6987.
(27) Kaplan, I. G.; Santamaria, R.; Novaro, O. *Int. J. Quantum Chem. Symp.* **1993**, *27*, 743.
(28) Jeschke, H. O.; Garcia, M. E.; Bennemann, K. H. *Phys. Rev. A* **1996**, *54*, R4601.
(29) Jeschke, H. O.; Garcia, M. E.; Bennemann, K. H. *J. Phys. B* **1996**, *29*, L545.
(30) Wedum, E. E.; Grant, E. R.; Cheng, P. Y.; Willey, K. F.; Duncan, M. A. *J. Chem. Phys.* **1994**, *100*, 6312.
(31) Wallimann, F.; Frey, H.-M.; Leutwyler, S.; Riley, M. *Z. Phys. D* **1997**, *40*, 30.
(32) Bonacic-Koutecky, V.; Cespiva, L.; Fantucci, P.; Koutecky, J. *J. Chem. Phys.* **1993**, *98*, 7981. Bonacic-Koutecky, V.; Cespiva, L.; Fantucci, P.; Pittner, J.; Koutecky, J. *J. Chem. Phys.* **1994**, *100*, 490.
(33) Hay, P. J.; Wadt, W. R. *J. Chem. Phys.* **1985**, *82*, 270, 299.
(34) Barandiaran, Z.; Seijo, L.; Huzinaga, S. *J. Chem. Phys.* **1990**, *93*, 5843.
(35) Moore, C. E. Atomic Energy Levels, Circ. No. 467, Nat. Bureau Standards, 1958; Vol. III.
(36) Desclaux, P. *At. Data Nucl. Data Tables* **1973**, *12*, 311.
(37) Bobrowicz, F. W.; Goddard, W. A., III. In *Modern Theoretical Chemistry: Methods of Electronic Structure Theory*; Schaefer, H. F., III, Ed.; Plenum: New York, 1977; Vol. 3, Chapter 4.
(38) Jaguar v3.0, Schrödinger, Inc., Portland, OR, 1997.
(39) Roos, B. O. *Int. J. Quantum Chem. Symp.* **1980**, *14*, 175.
(40) Dupuis, M.; Johnston, F.; Marquez, A. "HONDO 8.5 from CHEM-Station", IBM Corp., Neighborhood Road, Kingston, NY, 12401, 1994.
(41) Swope, W. C.; Andersen, H. C.; Berens, P. H.; Wilson, K. R. *J. Chem. Phys.* **1982**, *76*, 637.
(42) Gibson, D. A.; Ionova, I. V.; Carter, E. A. *Chem. Phys. Lett.* **1995**, *240*, 261.
(43) Kozlowski, P. M.; Davidson, E. R. *J. Chem. Phys.* **1994**, *100*, 3672.
(44) Andersson, K.; Malmqvist, P.-Å.; Roos, B. O.; Sadlej, A. J.; Wolinski, K. *J. Phys. Chem.* **1990**, *94*, 5483. Andersson, K.; Malmqvist, P.-Å.; Roos, B. O. *J. Chem. Phys.* **1992**, *96*, 1218. Merchan, M.; Serrano-Andres, L.; Gonzalez-Luque, R.; Roos, B. O.; Rubio, M. Theoretical spectroscopy of organic systems. *THEOCHEM* **1999**, *463*, 201−210.
(45) Herzberg, G. *Molecular Spectra and Molecular Structure III. Electronic Spectra and Electronic Structure of Polyatomic Molecules*; Van Nostrand Reinhold Co.: New York, 1966; p 341.